EMG sensing for Dual Control of Unicycle Robot

MANUEL MADEIRA, MARIA TERESA PARREIRA

Signal Acquisition Instrumentation in Bioengineering, Instituto Superior Técnico, Lisboa Portugal

Abstract: Over the last decades, the field of EMG based interfaces has received increased attention due to their cross-disciplinary. Among many applications, EMG can be used to translate activation of human muscles into commands understandable and executable by a robot artifact. The project presented in this report concerns the control of a platform robot, Pioneer P3-DX, via two EMG setups, each placed on the bicep of one arm, allowing for full, remote control on a 2D-space. We present the methods and pipeline used, which includes signal acquisition, a hardware component of amplification,filtering and rectification, the integration of this signal into a computer and further processing, as well as the remote communication of the outputs into commands for the robot. A comparison of the gains in the experimental settings with the simulated gains and theoretical gains reveals a higher experimental gain in the Differential Amplifier stage but a smaller gain in the Bandpass filter. Noise, stemming from the nature of the input signal (inherent instability of the EMG signal due to the approximately random nature of the firing rate of muscular motor units) and from the electronic components in the detection and recording instruments, and especially the electrodes used to capture the signal, is a great factor for decreasing of robustness in the system. Nonetheless, control and trajectory following are successfully achieved, serving as a witness to the extremely large potential of EMG-based interfaces, in particular for rehabilitation or auxiliary technology purposes.

Keywords: biomechanics; position control; prosthetics; EMG-controlled robot; myoelectric commands; electromyography; biorobotics; electromyogram based control

1. Introduction

Electromyographic (EMG) testing involves evaluation of the electrical activity of a muscle and is one of the fundamental parts of the electrodiagnostic medical consultation. It requires a thorough knowledge of the anatomy of the muscles being tested, machine settings and the neurophysiology behind the testing. Currently, EMG has uses both as a research tool, in noninvasively recording muscle activation, and clinically in the diagnosis and assessment of nerve and muscle disease and injury as well as in assessing the recovery of neuromuscular function after nerve damage.[1]

Over the last decades, the field of EMG based interfaces has received increased attention due to its cross-disciplinary. The research goes well beyond applications in diagnosis; EMG transcends the field of Medicine in the sense that, due to its non-invasiveness and fairly easy detection methods, it can be processed and transduced into applications in a wide range of fields of investigation.

Robotics in one of the areas on which EMG is thriving as a control method or to serve as an interface. From teleoperation of robots with up to 6 degrees of freedom,[2] control of prosthetic or robotic limbs[3] (where it can be made as precise as to achieve control of individual fingers in a prosthetic hand[4]), control of exoskeletons,[5] whose potential for rehabilitation is a witness to how far the field of Biomechanics in robotics has come, and even for development of muscle computer interfaces (for human computer interaction),[6] EMG is undeniably a flexible, dynamic

and promising tool for human-based control in robotics.

The work presented in this paper concerns Human-Robot Interfaces (HRI) and uses EMG to control a unicycle, platform robot. The Pioneer P3-DX is a robotic wheeled base designed for autonomous navigation and it is the world's most popular mobile research platform. The robot benefits from a complete Robot Operating System (ROS) for the purposes of programming at will and its interface with software such as *MATLAB* is well-documented, with open-source code available. In addition to having several ways of connecting to sources of control (tether connection to computer, ethernet, serial connection with pc or onboard computer),[7] this platform has a wide range of hardware options in order to increase mobility, precision and interactivity - from robotized grippers and arms (with integrated support) to video cameras, ultrasonic motion sensor, etc., its complete purpose can be modulated to the task at hands easily.

2. Biomedical Background

2.1. Muscle activity

Skeletal muscle fibers can be considered twitch fibers, because they produce a mechanical twitch response for a single stimulus and generate a propagated action potential. Skeletal muscles are made up of collections of motor units (MUs) - smallest muscle unit that can be activated by voluntary effort - each of which consists of an anterior horn cell (or motoneuron or motor neuron), its axon, and all muscle fibers innervated by that axon. The constituent fibers of a motor unit are activated synchronously. Fig.1 is a representation of two motor units. When stimulated by a neural signal, each motor unit contracts and causes an electrical signal that is the summation of the action potentials of all of its constituent cells. This is known as the Single Motor Unit Action Potential (SMUAP or MUAP) and may be recorded using electrodes inserted into the muscle region of interest.

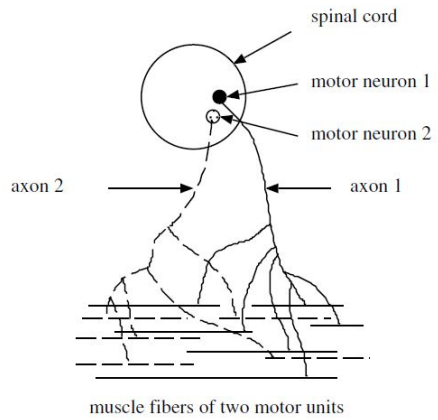

Fig. 1: Schematic representation of two motor units (one in solid line and the other in dashed line).[8]

The number of muscle fibers per motor nerve fiber (or motor unit) is known as the innervation ratio. While muscles for gross movement or large force have hundreds of muscle fibers per motor unit, muscles for precise or fine movement have fewer fibers per motor unit; in any case, the mechanical output (contraction) of a muscle is the net result of stimulation and contraction of several of its motor units. The innervation ratio can go from about 25 muscle fibers per motor

unit on the platysma to about 1934 muscle fibers per motor unit on the medial gastrocnemius (calf muscle of the leg).[8]

2.2. Acquisition - Surface EMG

EMG recordings make use of electrodes in order to convey muscle potential into an electrical, measurable one. Two main types of electrodes can be used:[9] needle electrodes (which are invasive but allow for the isolation of MUAPs) and surface electrodes, which were used in the present context.

Surface electrodes are typically either ring or disk electrodes and can be either disposable or non-disposable. The non-disposable electrodes are made of stainless steel, silver or gold, soldered to multistrand conducting wires. It is necessary to use conducting gel with non-disposable electrodes in order to reduce impedance and prevent artifacts (due to irregularities in the skin and the presence of hair follicles); on the other hand, disposable electrodes have a sticky underside that allows them to adhere to the skin generally without the need for tape or gel.

2.3. Electrode Placement

In order to acquire the best possible signal, EMG electrodes should be placed at a proper location - between the motor unit and the tendinous insertion of the muscle and along the longitudinal midline of the muscle, with the distance between the center of the electrodes or detecting surfaces being of around 1-2 cm.[10] Fig. 2 illustrates the electrode placement used in this project. This way, the detecting surfaces intersect most of the same muscle fibers and, as a result, an improved superimposed signal is observed. Additionally, the signal from the EMG detecting surfaces is gathered with respect to a reference, an electrode which acts as a ground for this signal and should be placed far from the EMG detecting surfaces, on an electrically neutral tissue such as bone (in this case, humerus or ulna are the best options, namely around the olecranian region).

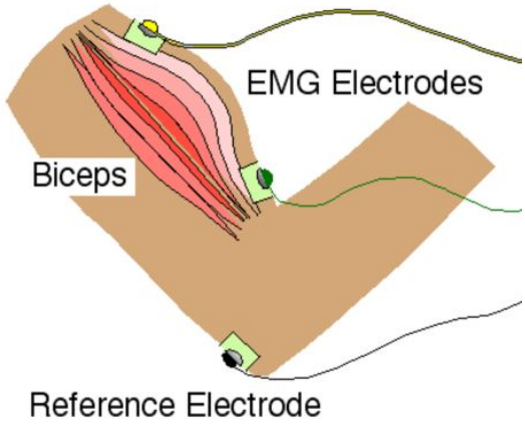

Fig. 2: Schematic representation of electrode placement in an EMG. Three surface electrodes are typically used: active and reference recording electrodes and a ground electrode. Retrieved from *EMG Sensing Circuit* (accessed on 10/06/2019).

2.4. Characteristics of Signal Acquired

Normal SMUAPs are usually biphasic or triphasic, with 3-15 ms in duration and 100-300 μV in amplitude.[8] On the other hand, the amplitude of the EMG signal is within a range from the μV to low mV (0-6 mV peak-to-peak). The energetic distribution of EMG signal is basically within the 0 to 500Hz range in frequency domain, with the dominant components in the 50-150 Hz range.[10,11]

One common problem with any acquisition of signal, and in particular of biomedical signals, is noise. In the case of EMG, signal acquisition can be said to be contaminated with four main sources of noise: **a)** inherent noise of electronic components in the signal detection and recording instruments; **b)** ambient noise from the electromagnetic radiation in the environment; **c)** motion artifacts with electrical signals, mainly in the frequency 0-20 Hz range, from the electrode-skin interface and from movement of the cable connecting the electrode to the amplifier, and finally **d)** the inherent instability of the EMG signal due to the approximately random nature of the firing rate of muscular motor units.

Of course, one should also mention inter-subject variability. Amplitude, time and frequency of EMG signals are influenced by the anatomical and physiological characteristics of muscles, the control mechanism of the nervous system, and the instrumentation involved. The timing and intensity of muscle contraction, the distance from the electrode to the target muscle, the amount of adipose tissue between the skin and the muscle and the quality of the contact between the skin and the electrode are factors that cause variability in the signal measured.[12]

3. Methods

In order to accomplish a correct acquisition of the EMG, the signals transduced by the electrodes are the input to a processing circuit. The first stage consists of a differential amplifier, followed by a stage of filtration. After these two steps, a full wave precision rectifier with a low-pass filter in its end is applied.

After this stage, a hardware amplification, filtering and processing, the signal obtained is integrated and digitized by a *Arduino* device, allowing its direct implementation in *Matlab* software. The signal obtained is then "translated" into information on how the robot is intended to behave and this command is transferred via a TCP-IP connection with another computer, which is effectively physically connected to the Pioneer P3-DX. This second computer gives controls to the robot according to the information it has just received.

The pipeline explained above is illustrated in Figure 3.

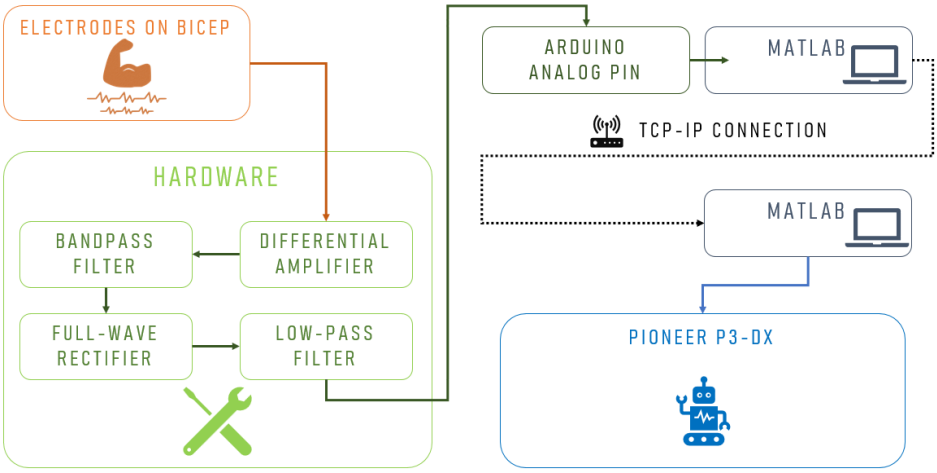

Fig. 3: Pipeline of the approach adopted to control a Pioneer P3-DX through an EMG acquisition.

3.1. Hardware

3.1.1. Electrodes

In order to transduce the physiological signal into an electric one (*i.e.* convert muscular activity into voltage and/or intensity), we used two sets of electrodes (one for each arm) which were available in the laboratory and can be seen in Fig.4.

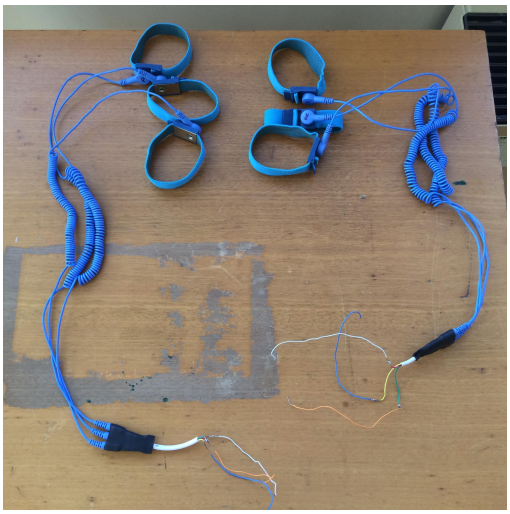

Fig. 4: Electrodes used to transduce the physiological signal into an electrical, able to be processed signal.

The electrodes used are surface electrodes, which constitute a non-invasive technique for measurement and detection of EMG signal, though generally used for superficial muscles only with a big probability of cross-talk with other muscles. The underlying working principle of those electrodes comes from a chemical equilibrium between the detecting surface and the skin of the

body through electrolytic conduction, so that current can flow into the electrode.[10] Consequently, these electrodes are simple and easy to implement - a strict medical supervision and certification isn't required, contrarily to what happens in the case of needle or fine wire electrodes. More precisely, they fit into the category of dry electrodes - they do not require a gel interface between skin and the detecting surface, introducing more electrical noise into the measurement, when compared with the equivalent gelled electrodes, and are heavier, causing an increased inertial mass, which may cause problems for electrode fixation; therefore, a material for stability of the electrode with the skin is required - and passive electrodes - they require a connection to an external amplification circuitry with the help of connecting wires for the proper acquisition of the EMG signal.[10]

The acquisition of the physiological signal is based on the simple fact that whenever a muscle contracts, a burst of electric activity is generated, propagating through adjacent tissue and bone. Consequently, this signal can be recorded from neighboring skin areas, which is where the electrodes are placed. Since in our approach a differential amplifier is used as the first stage (procedure which is commonly used in EMG, as previously mentioned), three electrodes are applied in each arm: two of them are placed along the bicep muscle, catching the muscular activity itself, and another one (reference) is placed on a bony region (near the elbow and/or ulna). The regions where the electrodes are placed aren't absolute since there's high variability among different individuals and, more importantly, we are more concerned in obtaining a binary signal (signal/no signal) than a uniform and reproducible one.

3.1.2. Differential Amplifier

As previously mentioned, after the acquisition of the signal, it goes through a processing circuit, whose first stage is a differential amplifier with the main aim of rejecting the common mode as much as possible, while amplifying the differential one. The circuit used to achieve this is represented on Fig.5.

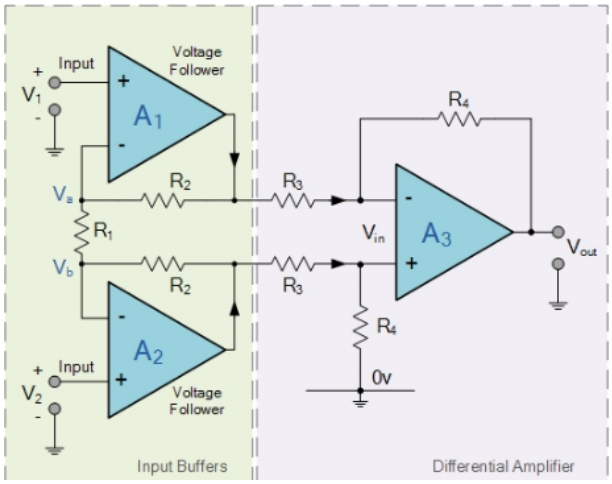

Fig. 5: Scheme of the circuit applied as differential amplifier (1st stage of the processing circuit). Retrieved from ElectronicsTutorial, *High Input Impedance Instrumentation Amplifier* (accessed on 10/06/2019).

The instrumentation used in the circuit above has the capability of imposing a high input impedance. Moreover, v_{out} can be obtained from v_1 and v_2 by the following expression:

$$v_{out} = -\frac{R_4}{R_3} \times (1 + 2 \times \frac{R_2}{R_1}) \times (v_1 - v_2), \tag{1}$$

where the factor $(1 + 2 \times \frac{R_2}{R_1})$ results from the 1st stage ("Input Buffers") and the factor $-\frac{R_4}{R_3}$ results from the 2nd stage ("Differential Amplifier" itself).

3.1.3. Filtration

In order to filter the signal, two Sallen & Key filters were used (a high-pass one, followed by a low-pass), in order to achieve a band-pass filtration. The used filters are represented in Fig.6.

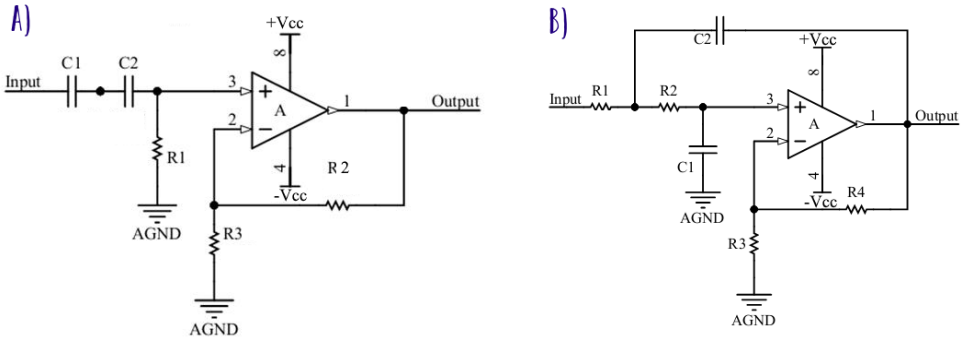

Fig. 6: Scheme of the analogic filters used in the circuit (2nd stage of the processing circuit). Adapted from Wang *et al.* (2013)[11]

The transfer function of the circuit A) is given by:

$$H(s) = k \times \frac{sCR_1}{sCR_1 + 1}, \tag{2}$$

where $C^{-1} = C_1^{-1} + C_2^{-1}$ and $k = \frac{R_3 + R_2}{R_3}$, which is the gain for frequencies after the pole.

Thus, the pole of this high-pass filter is given by: $f_{HPP} = \frac{1}{2\pi \times CR_1}$, having a zero at $f_{HPZ} = 0$.

Regarding the low-pass filter, it is a 2nd order filter, whose transfer function is given by the following equation:

$$H(s) = \frac{k}{s^2(R_1C_1R_2C_2) + s(C_1R_1 + R_2C_1 + R_1C2(1-k)) + 1}, \tag{3}$$

where $k = 1 + \frac{R_4}{R_3}$, which is the gain before the poles start to exert their influence on the transfer function.

Thus, the corner frequency for this filter can be obtained:

$$f_C = \frac{1}{2\pi\sqrt{R_1R_2C_1C_2}}, \tag{4}$$

The strategy of using two filters leading to a band-pass filters motivated by the the main components of the EMG signal being within the 50-150Hz band, as was mentioned before. Moreover, it's safe to assume that power supply-based noise, with a dominant frequency of 50Hz,

would affect the signal and it's effect would worsen after the amplification stage . Consequently, our approach intended to keep only frequencies above that value while simultaneously keeping out high frequencies, completely outside of the intended range. Further explanations are detailed on Section 3.1.5.

3.1.4. Full Wave Precision Rectifier and Low-Pass Filter

The next step consisted of rectifying the signal, *i.e.*, converting the signal into its absolute value, since the *Arduino* retrieves signal between 0V to 5V. The strategy used is a Full-Wave Precision Rectifier, which is represented on Fig.7.

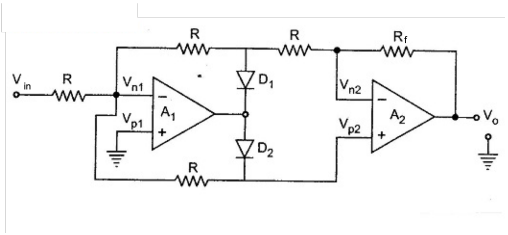

Fig. 7: Scheme of the circuit applied as Full-Wave Precision Rectifier (3rd stage of the processing circuit). Retrieved from EEGGUIDE.COM, *Precision Full Wave Rectifiers*. Accessed on 10/06/2019.

This stage includes a small modification from the standard Full Wave Rectifier Circuit, since resistor R_f has a different value in comparison with the remaining resistors of this circuit. As a consequence, the equations ruling this Rectifier become:

$$\text{if} v_{\text{in}} > 0 : v_o = \frac{R_f}{R} \times v_{\text{in}} \tag{5}$$

$$\text{if} v_{in} < 0 : v_o = (-\frac{2}{3} - \frac{1}{3} \times \frac{R_f}{R}) \times v_{in} \tag{6}$$

The reason for this modification is properly detailed in Section 3.1.5.

Lastly, since the main aim is to give discrete orders to a robot, we're not interested in the small oscillations of our signal (which are typical of a pure EMG signal); therefore, a capacitor was inserted in parallel with R_f, allowing the circuit to have an output similar to a trend of the signal, instead of following it in a strict way.

3.1.5. Final Circuit

In order to not only size each of the different components of the circuit more quickly but also have an graphical idea of its transfer function, we resorted to the *LTSpice* software. Fig.8 shows the total circuit used, while the transfer function is shown in Fig.11, Section 3.1.5.

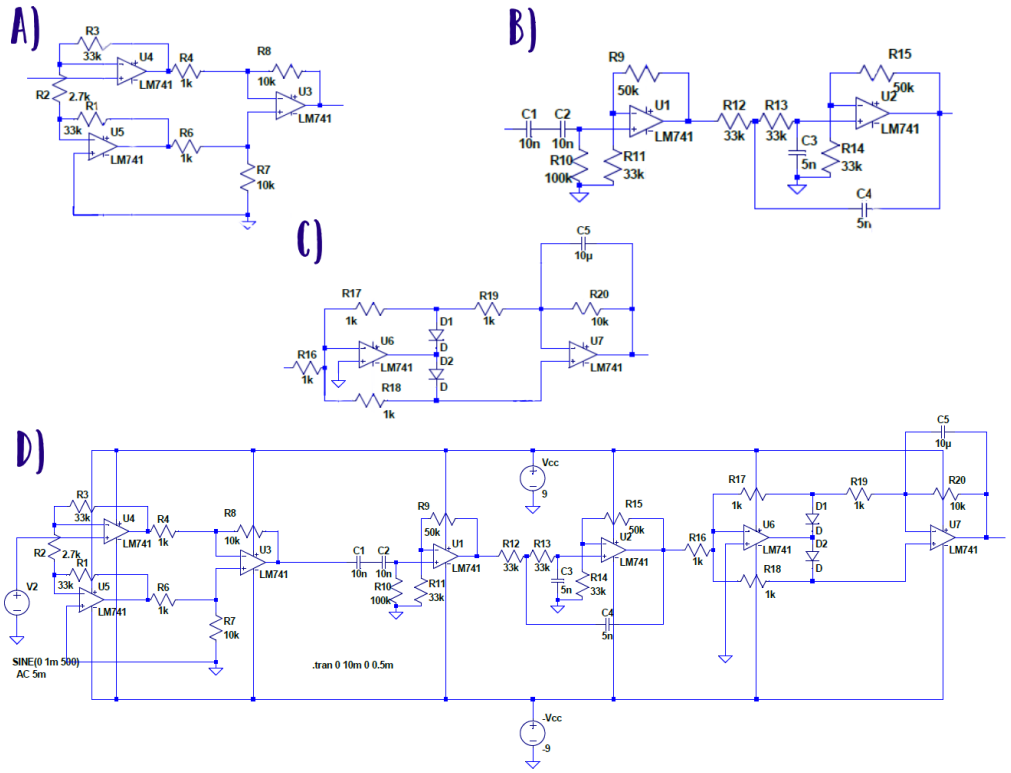

Fig. 8: Schemes of the implemented circuits in the *LTSpice* software, as well as the value of each of the components used: A) Differential Amplifier with High Input Impedance; B) Filtration Stage (Active 1st Order High-Pass Filter and Sallen-Key Low-Pass Filter); C) Rectifier and Low-Pass Filter; D) Total Circuit.

From the theoretical point of view and accordingly to what was mentioned in previous sections, the different parameters which more comprehensively describe the behaviour of this circuit can be computed by replacing each variable by the values as seen in the figure above:

A) Differential Amplifier:

$$v_{out} = -\frac{10k\Omega}{1k\Omega} \times (1 + 2 \times \frac{33k\Omega}{2.7k\Omega}) \times (v_1 - v_2) \approx -254.44(v_1 - v_2) \tag{7}$$

B1) Filtration - High-Pass Filter:

$$f_{HPP} = \frac{1}{2\pi \times 100k\Omega \times ((10\mu F)^{-1} + (10\mu F)^{-1})^{-1}} = 318.31Hz \tag{8}$$

$$k = \frac{33k\Omega + 50k\Omega}{33k\Omega} \approx 2.52 \tag{9}$$

B2) Filtration - Low-Pass Filter:

$$f_C = \frac{1}{2\pi \times \sqrt{33k\Omega \times 33k\Omega \times 5\mu F \times 5\mu F}} = 964.58Hz \tag{10}$$

$$k = 1 + \frac{50k\Omega}{33k\Omega} = \approx 2.67 \tag{11}$$

Overall, for signal components whose frequency is between f_{HPP} (318.31 Hz) and f_C (964.58 Hz) the gain will result from the multiplication of both gains, yielding an overall gain $K_{overall} \approx 6.73$.

C) Full-Wave Precision Rectifier

$$if\ v_{\text{in}} > 0 : v_o = \frac{10k\Omega}{1k\Omega} \times v_{\text{in}} = 10v_{\text{in}} \tag{12}$$

$$if\ v_{in} < 0 : v_o = (-\frac{2}{3} - \frac{1}{3} \times \frac{10k\Omega}{1k\Omega}) \times v_{in} = -4v_{in} \tag{13}$$

One point that should be stated is that this relation between v_o and v_{in} is being considered independent of the frequency of the signal, which isn't completely true. The capacitor responsible for low-pass filtering the response introduces a frequency-dependent component on the transfer function of this stage, which isn't being considered in the expressions above.

Nevertheless, taking into account that the amplitude of the EMG signal is within a range from the μV to low mV (0-6 mV peak-to-peak or 0-1.5 mV RMS),[11] and given the amplification already mentioned in the first two stages ($254.44 \times 6.73 \approx 1712$), it's almost certain that the EMG signal will lead to the saturation of the Operational Amplifiers after this last stage. We should add that we're dealing with the higher frequency components of the EMG as a result of our filter choice, and therefore, we should expect to amplify EMG components whose amplitude is usually smaller when in comparison with the EMG components within the main band of frequencies of interest.

This circuit is duplicated so that we're able to get information coming from both biceps of the patient (one circuit for each arm). The real circuits are represented on Fig.9.

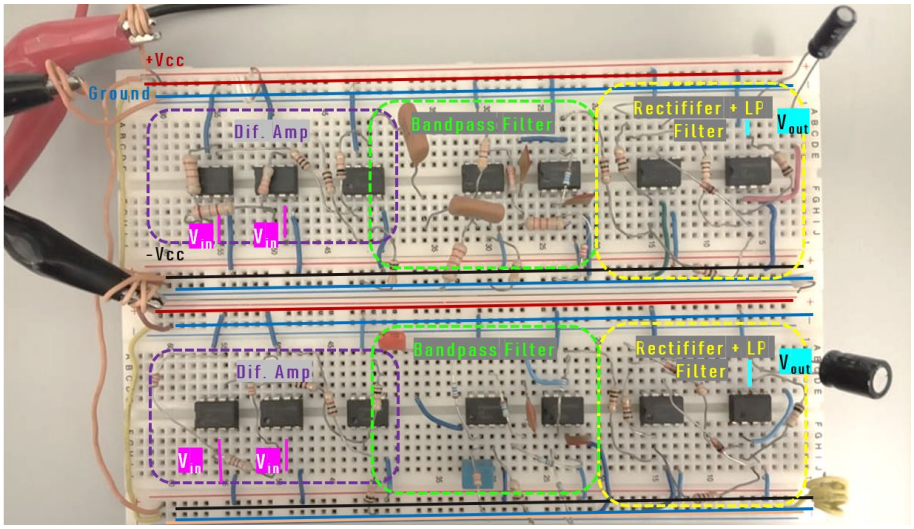

Fig. 9: Real circuits used to process the signal. Each of the breadboards has one of the circuits mentioned previously, able to receive and process the EMG signal of one bicep.

The processed EMG signal is collected on the v_{out} nodes, represented on Fig. 9, with each of them being connected to two different Analog Pins of Arduino (A0 and A2).

3.2. Software

3.2.1. Signal Integration on *Matlab*

The outputs of each of the two EMG circuits are then integrated using the Analog Pins in *Arduino*, which can be read directly via *Matlab*. The signal is processed in a very quick-to-compute, simple way, as most preprocessing is done via hardware stages. A threshold in amplitude is defined and, if the signal exceeds it, a binary command variable becomes 1; if not, command is set to 0.

Two thresholds are defined, one for each arm, as well as three "command" variables (one for the right arm, one for the left arm, both binary, and a third, general command). The thresholds are determined empirically and the need for two is justified by differential strength in each arm. The binary commands will reflect in a general command, which is communicated to the robot. Its determination is detailed in Table 1

Table 1: Relation between each of the binary commands (right or left) and general command. Action determined by each value assumed.

Right Command	Left Command	General Command	Action
0	0	0	Stop
1	1	1	Move Straight
1	0	2	Turn Right while Stopped
0	1	3	Turn Left while Stopped

3.2.2. PC-to-PC Communication and Integration to Robot

Using *Matlab*, it's possible to establish a TCP-IP connection between two computers connected to the internet. The computer connected to the hardware, where the signal is processed into the general command explained before, communicates that variable to a computer connected via serial connection to the robot Pioneer P3-DX. The maximum duration of this communication needs to be pre-determined and for the experiments in the present project was set at 200s (of course, it can be interrupted prematurely).

According to the value of the command received, the robot will either stop (linear velocity v and angular velocity ω equal to 0), move straight ($v = 250$ mm/s, $\omega = 0°/s$) or rotate ($v = 0$ mm/s, $\omega = \pm 20°/s$).

A consistency variable was included, in order to guarantee that a single measure above or below the threshold would not cause a change in the command variables - otherwise, the command would oscillate and the robot's motion would be unstable. The strategy, again, was simple and of very demand for little computational resources: from the moment when a measure above the threshold falls below it, or vice-versa, a counter variable is updated by summing 1 to its value. If it reaches a certain number, *e.g.* 5, the binary command gets changed. However, if a new measure returns a value consistent with the current command (*i.e.* if command is 1 and new amplitude is above threshold or if command is 0 and new amplitude is below threshold), then the counter is reset to 0 and there are no binary command changes. There is, however, a trade-off between consistency and delay of control: if the counter threshold is too high, the shift in controls will take a long time.

Note that the consistency and commands had to be strategically thought as instantaneously processed approaches: because the signal is constantly being updated and needs to be translated into controls with a minimum delay, a lot of processing techniques had to be excluded because of their dependency on many previous or even future values of the signal.

4. Results and Discussion

4.1. Sinusoidal input

In order to test the different stages of the circuit built, a simulation was carried out on the software *LTSpice IV*. Following this stage, the experimental setup was tested under the same conditions. Results for one of the inputs as ground and the other with a sinusoidal input, $v_{pp} = 1mV, f = 500Hz, V_{\text{offset}} = 0V$, can be seen in Fig. 10 and will be detailed below.

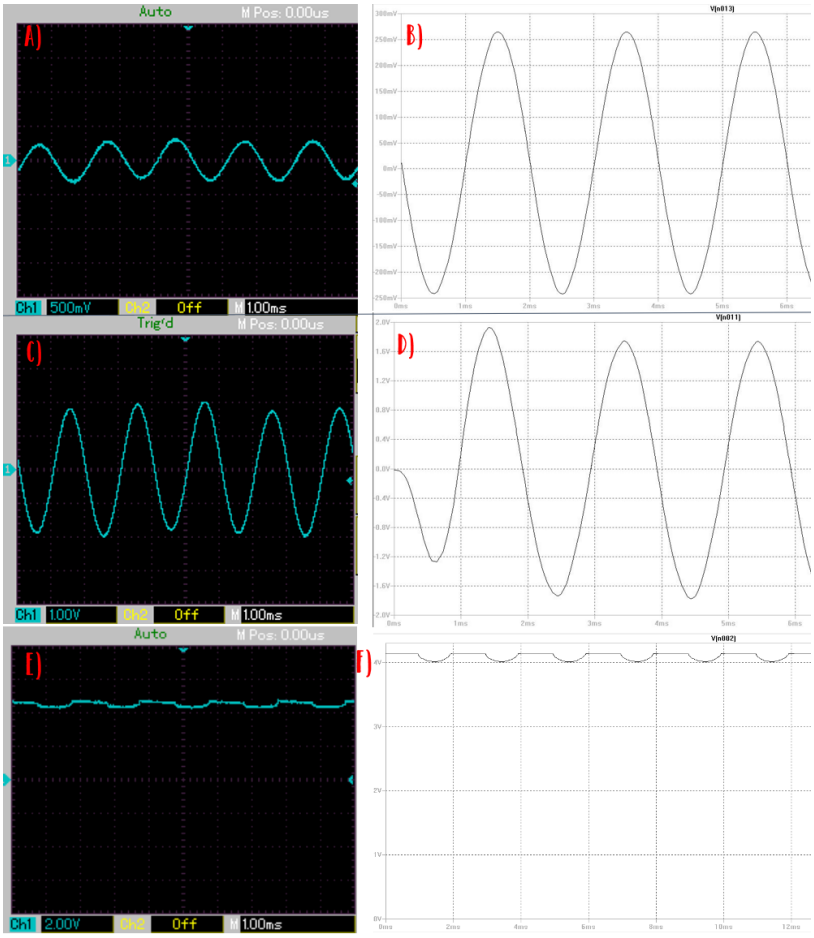

Fig. 10: Simulated and experimental results of EMG circuit. **A)** Output of differential amplifier, measured after C1 (Fig.8-D)), in experimental circuit; **B)** Simulated output with respect to A); **C)**Output of bandpass filter, measured after R15 (Fig.8-D)), in experimental circuit; ; **D)** Simulated output with respect to C); **E)** - Output of wave rectifier, measured after R20 (Fig.8-D)), in experimental circuit; **F)** Simulated output with respect to E);

In this case, $+V_{cc} = 5.1V, -V_{cc} = -4.9V$, due to the fact that, experimentally, the voltage source was unable to produce completely symmetric outputs. For the Differential Amplifier stage, on the oscilloscope maximum amplitude was measured as 290mV - a gain of 290 - whereas the simulation presented a gain of 264. From the theoretical point of view, the expected gain was 254, approximately, as mentioned previously, resulting in an error of 14.17% and 3.94% in the experimental and simulated gains. These results can be easily explained by the imperfections of real components when compared with the idyllic behaviour assumed on the theoretical approach. The *LTSpice* software already takes into account some imperfections (*e.g.* output voltage offset and other properties of real OpAmps are considered in OpAmps models of the mentioned software) and, so, it isn't surprising that the results of this approach show an intermediate behaviour between the real and the theoretical ones.

The bandpass filter also includes a gain component. The value measured on the oscilloscope for maximum amplitude was on average 1.83V, which would correspond to a gain of 6.31 of the output from the previous stage (differential amplifier), but of 1830 in regards to the input of the circuit. On its turn, the simulation calculates a maximum amplitude of 1.74V, which corresponds to gains of 6.59 and 1740 with respect to output of amplifier stage and input of circuit, respectively. One of the explanations for a higher gain in the simulation is the values of R9 and R15, which are set as $50k\Omega$ but actually correspond to $46.7k\Omega$, as well as for the capacitors C3 and C4, whose real values are $5.6nF$. Therefore, the simulated gain will be calculated as being higher. If this is corrected, the simulated gain becomes 6.28, which is close to the one observed experimentally. The theoretical gain is, as was mentioned, of 6.73, calculated for the electronic components as they are simulated. Therefore, the error in relation to the simulation is of 2.08%, easily justified by the deviation from the nominal values of resistances as well as from the approximation to ideal Op Amp in calculations.

Finally, the results in the final stage, the Full Wave Precision Rectifier, can be explained by the tension limiters $+V_{cc}, -V_{cc}$ and by the difference between them. This stage simultaneously rectifies the wave and passes it through a low-pass filter. In both the simulation and the experimental setup, the signal is amplified to the point of saturation (of the Op Amps). The negative part of the wave is then rectified to a positive value, which results in high-frequency variations in the signal. The low-pass filter embedded in the rectifier will smooth these transitions, resulting in very small oscillation around 5V (*i.e.* the power supplies of the Op Amps in the circuit). We hypothesize that, with a completely symmetrical power supply, we would observe an approximately straight line.

Of course, one must always keep in mind the non-ideality of electronic components, which is a huge source of deviations from theoretical calculations and even simulations, which already incorporate in calculations some of the discrepancies from the ideal cases. Some of the most common limitations in an EMG signal acquisition were already mentioned in Section 2, as possible sources of noise. Additionally, components such as resistors and capacitors deviate from their nominal value (*e.g.* a $10k\Omega$ resistor's real value only being $9.8k\Omega$);

4.2. Transfer Function

The transfer function of the processing circuit was generated using *LTSpice* for simulation so that a comparison with the theoretical expected behaviour could be accomplished and critically analysed. This transfer function is shown on Fig.11.

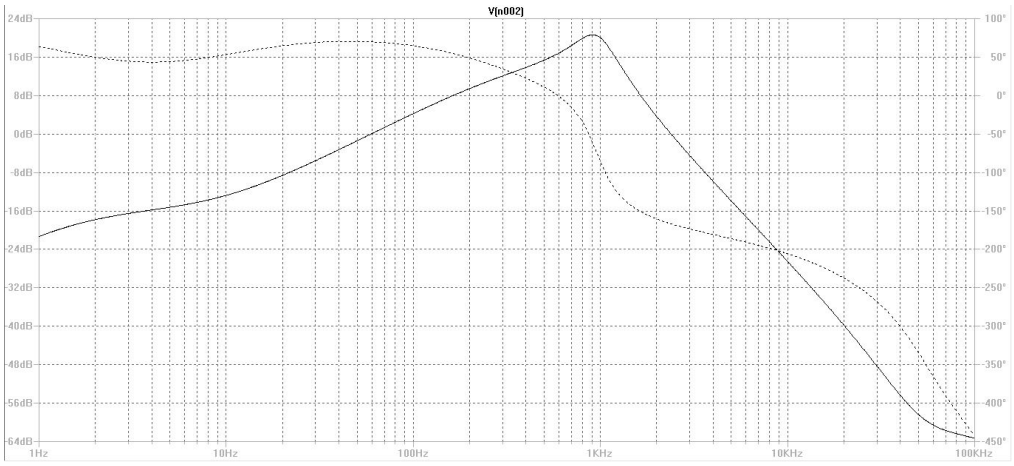

Fig. 11: Transfer function obtained through the *LTSpice* software. Scale: xx - Frequency (log(Hz)); yy - Amplitude(dB), line in black; Phase (°), dotted line.

In fact, analysing Fig.11, the behaviour shown by the system is more or less the expected: for frequencies below the passing band, the amplification increases at a rate of approximately 20dB/dec, since it's being cut by a 1st order high-pass filter (only one pole); after the passing band it decreases at a rate of approximately -40dB/dec, since it's being cut by a 2nd order low-pass filter (two poles).

There is a deviation from the predicted results, since the passing band is not identical to the theoretical expectation: the passing band doesn't extend from $f_{HPP} = 318.31Hz$ to $f_C = 964.58Hz$. Actually, there's no clear passing band, seeming that the two asymptotes just mentioned intersect each other. This result can be explained by the fact that, for some reason our $f_{HPP} = 318.31Hz$ isn't effectively on that frequency, leading to a continuously increasing |H(s)| until a frequency near of f_C. An hypothesis to this behaviour can be the influence of the OpAmps in the frequency response, even though we couldn't figure out a clear relation between these two points.

Although this was the simulated transfer function for our circuit, which is not the desired, experimentally the response was adequate and suited its purpose in amplifying and filtering the noise. This is the reason why the first filter was kept as a 1st order high-pass, since it allowed for the observation of a sufficiently clear EMG signal. This empirical observation can result from the fact that the filtration rate is able to successfully attenuate the 50 Hz noisy component introduced by the power supply, while keeping some of the lower frequencies component of the EMG signal.

4.3. Wave envelope

The analog to digital conversion of the signal is achieved using the Analog Pins A0 and A2 of an Arduino. This step of the pipeline carries some concerns related with the fact that the Arduino Analog Pins only consider voltages between 0 and 5 V or with the use of an inappropriate frequency of sampling (could cause aliasing, for example). However, given the fact that the EMG signal was rectified (though not in a typical way) and low-pass filtered in the last stage of the processing circuit, our approach is protected from those threats. The already digitized results are shown on Fig.12.

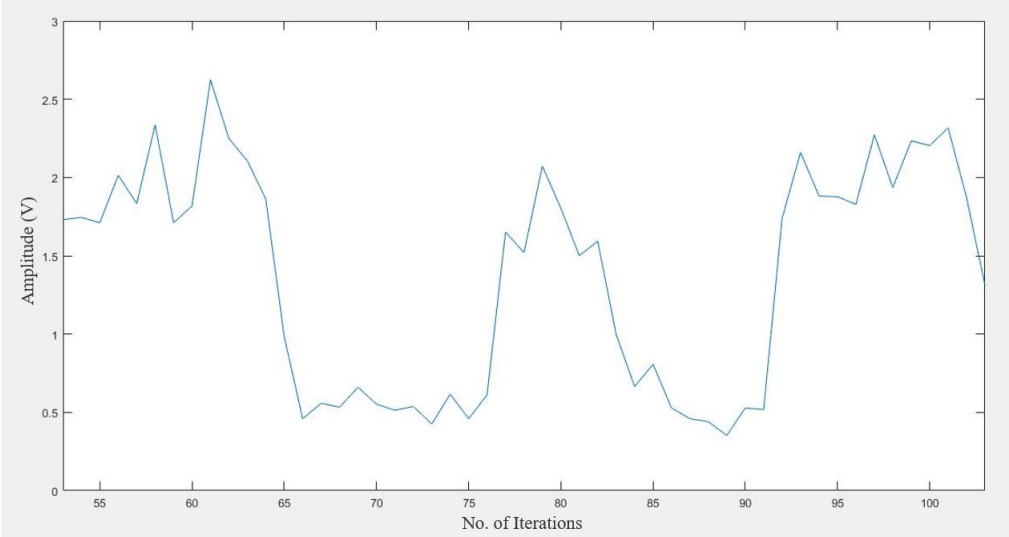

Fig. 12: Digital signal obtained from the conversion of the analog processed EMG into a digital one, through the Arduino Analog Pins. xx - number of iteration of signal retrieving cycle, in *Matlab*; yy - Amplitude (V)

Fig.12 shows three periods of muscular activation (no. of interations: beginning of the window to 65; 75 to 85 and 90 to the end of the window) and two of muscular relaxation moments of one arm/bicep (no. of interations: 65 to 75 and 85 to 90). Note that the basal activity of the muscle (*i.e.* during relaxation) has an amplitude that oscillates close to the value 0.5V. This results from the very high amplification of our circuit, eventually amplifying some electrical background activity as well. Nevertheless this feature, which was not projected initially, allowed us to understand whether the electrodes were working correctly or not, one of the main difficulties faced in this project (since absence of noise meant absence of contact between the electrodes and the rest of the circuit). After all, there's a clear difference on the amplitudes shown in for activation and relaxation moments, which was our main aim since it allows the binary codification of the activity of bicep.

4.4. Limitations

EMG circuits are well-known and a lot of literature can be found on how to build and optimize their function. However, in a Laboratory setting, with limited material and limited quality of that material, it's arduous to troubleshoot and understand fully where errors are stemming from. Deciding the design of each stage proved to be more complex than initially thought; for instance, when designing the Differential amplifier, both its stages were devised to have a 100 and a 10 gain, respectively. However, due to the occurrence of amplification of the difference between inputs on the first stage, we observed a large amplification of noise as well, after which the gain was decreased and divided more harmoniously between both the stages of the Amplifier and the Bandpass filter stage.

One must also refer limitations within the input acquisition, as the electrodes used often showed bad electrical contact or no contact at all. We point this out as the main obstacle to robustness in this project. Of course, the signal magnitude is partially dependent on electrode placement, as was discussed above and that was a primary concern. However, with the electrodes placed in a proper location, the input signal would very often oscillate in maximum amplitude

(under the same conditions) and regularly be contaminated with large noise and a large DC offset as a baseline, which is particularly concerning since the maximum amplitude would not increase linearly with the offset. Different offsets and different maximum amplitudes were observed, not only when simultaneously measuring both arms with different electrodes, but also in different moments in this. Note that these limitations were not constant within a circuit, *i.e.* it wasn't always the same circuit displaying the largest offset, for instance, which helps isolating the source of variations as being the electrodes and their connection. Additionally, signal was very sensitive to oscillations of the wires of the electrodes, which again increased the noise significantly. In short, this was probably the most time-consuming stage of the project and one we were, unfortunately, not able to successfully overcome.

One can also point out that one of the limitations in our approach was its susceptibility to muscle fatigue. For instance, in order to maintain the robot moving straight, both the left and right biceps must be in contracting with a magnitude above their threshold for the desired duration of the motion. This is a difficult task and leads to short duration of the forward motion command, due to the decrease in magnitude as a result of fatigue of the muscles. This is paradoxal, since muscle fatigue is actually physiologically translated as a bigger recruitment of muscle units, that is, a higher shooting rate. Of course, choosing the bicep, a large muscle, as the source of signal, increases the noise in the signal (when compared to smaller muscles), but this is not a very remarkable limitation as our purpose was the collection of a signal only robust enough to be transformed into a binary variable.

5. Conclusion

EMG based interfaces, which can be used to decode human intention and estimate human kinematics using the myoelectric activity captured from human muscles, are a promising area of research and EMG control schemes will probably have a vital role in human robot/computer interaction applications in the future, but they currently still carry several issues, inherent to dealing with the high-dimensionality and complexity of the human musculoskeletal system, the non-stationarity of the EMG signals and the non-linear relationship between the human myo-electric activity and the motion or force to be estimated.

In the case of this project, discrete but dual control was used, allowing for four distinct commands and thus providing total mobility in a 2D space to the platform robot used. Additionally, the controls are provided remotely, which is a feature of great importance for applications in cases of low mobility, and rely on wi-fi connection, which is typically robust and can be used for considerable distances.

An interesting extension of this project would be to incorporate the video from the webcam on the computer placed on the robot and stream it into the pc next to the operator individual - this would allow for complete remote control and could easily be achieved via streaming directly on *Matlab* (although this would probably induce a lot of delay into the communication) or using a different software solely for the purpose of video streaming, which would act as visual feedback (the current approach contains visual feedback but it is limited to the field of view of the operator).

As was mentioned in the Introduction, the Pioneer P3-DX is a robot who possesses the great advantage of being easily adjustable to the specifications of a task, since it can very easily have add-ons of various origins and purposes. Therefore, apart from a camera, robotic arms can be added for precise and remote control, for instance. In general, we point out as main potential biomedical applications of this project the possibility of auxiliary technology (**e.g.** in cases of reduced mobility), in interactive therapy (*e.g.* to help autistic children interact in a dynamic way) or in rehabilitation, as a dynamic form of muscle training while acquiring physiological data.

EMG based interfaces are definitely a field of ever-growing interest and further approaches will probably abandon the current paradigm, which involves training an individual to control a robotic artifact, to a paradigm where the robot adapts its controls to human response, *i.e.* through data handling and machine learning, the robot is trained to respond to the most reliable or best performing controls; this constitutes yet a step further in personalized Health/Medicine.

References

1. S. M. Roe, C. D. Johnson, and E. A. Tansey, "Investigation of physiological properties of nerves and muscles using electromyography," Adv. Physiol. Educ. **38**, 348–354 (2014).
2. J. Vogel, C. Castellini, and P. van der Smagt, "EMG-based teleoperation and manipulation with the DLR LWR-III," in *2011 IEEE/RSJ International Conference on Intelligent Robots and Systems,* (2011), pp. 672–678.
3. C. Cipriani, F. Zaccone, S. Micera, and M. C. Carrozza, "On the Shared Control of an EMG-Controlled Prosthetic Hand: Analysis of User-Prosthesis Interaction," IEEE Transactions on Robotics **24**, 170–184 (2008).
4. J. Zhao, Z. Xie, L. Jiang, H. Cai, H. Liu, and G. Hirzinger, "EMG Control for a Five-fingered Underactuated Prosthetic Hand Based on Wavelet Transform and Sample Entropy," in *2006 IEEE/RSJ International Conference on Intelligent Robots and Systems,* (2006), pp. 3215–3220.
5. H. He and K. Kiguchi, "A Study on EMG-Based Control of Exoskeleton Robots for Human Lower-limb Motion Assist," in *2007 6th International Special Topic Conference on Information Technology Applications in Biomedicine,* (2007), pp. 292–295.
6. S. Saponas, D. Tan, D. Morris, and R. Balakrishnan, "Demonstrating the Feasibility of Using Forearm Electromyography for Muscle-Computer Interfaces," (ACM, 2008), pp. 515–524.
7. A. R. C. MobileRobots Exclusive and O. Software, "Pioneer 3 Operations Manual," (MobileRobots Inc., 2006).
8. R. M. Rangayyan, *Biomedical Signal Analysis, Second Edition* (Wiley - IEEE Press, 2015).
9. L. Weiss, J. Weiss, and J. Silver, *Easy EMG: A Guide to Performing Nerve Conduction Studies and Electromyography* (Elsevier Health Sciences, 2015).
10. M. Z. Jamal, *Computational Intelligence in Electromyography Analysis - A Perspective on Current Applications and Future Challenges* (InTechOpen, 2012).
11. J. Wang, L. Tang, and J. E. Bronlund, "Surface emg signal amplification and filtering," (2013).
12. C. J. D. Luca, "Surface electromyography: Detection and recording," (2002).